Screening of Lost Circulation Materials for Geothermal Applications: Experimental Study at High Temperature

Cesar Vivas[1]
Mewbourne School of Petroleum and Geological Engineering,
The University of Oklahoma,
Norman, OK 73019-1003
e-mail: cesar.vivas@ou.edu

Saeed Salehi
Mewbourne School of Petroleum and Geological Engineering,
The University of Oklahoma,
Norman, OK 73019-1003
e-mail: salehi@ou.edu

This study presents a laboratory experimental research to determine the characteristics of lost circulation materials (LCMs) capable of addressing thermal degradation, providing bridging and sealing in geothermal conditions. Eleven different materials were tested: Walnut Fine, Walnut Medium, Sawdust, Altavert, Graphite Blend, Bentonite Chips, Micronized Cellulose (MICRO-C), Magma Fiber Fine, diatomaceous earth/amorphous silica powder (DEASP), Cotton Seed Hulls, and a Calcium Carbonate Blend. The filtration and sealing pressure of the LCMs were measured with HPHT equipment up to 149 °C (300 °F). Besides, the particle size distribution (PSD) of fine granular materials was measured. The results show that the performance of some LCM materials commonly used in geothermal operations is affected by high temperature. Characteristics such as shape and size made some materials more prone to thermal degradation. Also, it was found that the PSD of LCMs is a key factor in the effectiveness of bridging and sealing fractures. The results suggest that granular materials with a wide particle size distribution PSD are suitable for geothermal applications. [DOI: 10.1115/1.4053071]

Keywords: lost circulation materials, HPHT filtration, fracture sealing, geothermal drilling, particle size distribution, geothermal energy

1 Introduction

Lost circulation is caused by mud entering into porous or fractured rock, causing the reduction in the hydrostatic column (mud column). The mud is getting into the formation instead of returning to the surface [1]. The mud loss is the most serious problem during the drilling of geothermal wells, mainly due to its high frequency and associated high costs. The temperatures found in geothermal fields cause a reduction in rock strength [2]. Besides, complex fracture networks are common in geothermal reservoirs [3]. Also, the temperature increase with the geothermal gradient increases the likelihood of mud invasion in the exposed wellbore [4]. The highly fractured rock environment found in geothermal drilling is one of the most common causes of massive mud loss events. Fractures that measure 1000–3000 μm or more are complicated to cure at high temperatures. If not controlled, mud losses can lead to impacting issues such as stuck pipe events or well-integrity issues [5–7]. Although this phenomenon has been extensively studied, lost circulation is still the most problematic and costly issue in geothermal drilling [6].

In typical geothermal wells, mud losses often correspond to a significant portion of non-productive time (NPT). Cole et al. [8] analyzed data from 38 geothermal wells drilled in the United States since 2009. The study found that wells accumulated more than 100 h of non-productive time on average due to loss of circulation, contributing to rig costs of an additional $185,000 or more per well. In a typical geothermal well, mud losses account for 20% of the total costs [9].

Problems related to mud losses in geothermal operations have been documented since the 1970s; however, the difficulties depicted are still not fully solved. Marbun et al. [10] described how operational problems associated with mud losses and stuck pipe events, causing the operational drilling times to be four times the amount of time initially planned in a field in Indonesia. Pálsson et al. [11] described how non-controlled mud losses prevented the planned well depth from being reached in the Krafla field, Iceland. In this operation, multiple sidetracks were attempted, but the loss of circulation did not allow reaching the planned target. Bolton et al. [12] described how total losses caused a well control event in the Wairakei field, New Zealand. To stop the blowout, a relief well to intercept the uncontrolled well was drilled. In Imperial Valley (California, USA), lost circulation zones are present anywhere along the wellbore [13]. LCM is traditionally used to restore mud returns. Mud losses are typical in The Geysers, California [14]. Highly fractured, localized zones characterize loss circulation areas. Cottonseed hulls were reported to be the most commonly used LCM, and 12 ppb was a typical concentration to address losses. Occasionally, when mud circulation could not be restored, cement was used to cure mud losses.

Nuckols et al. [15] described a severe loss of circulation event in Fenton Hills (Jemez Mountains, Northern New Mexico). Several attempts to cure losses were performed, including the circulation of bridging agents (1500 bbl of LCM at 30% of volume), and cementing jobs were performed without success. Finally, it was decided to drill without returns and run the casing to isolate the loss sections. The consequences of mud losses were stuck pipe events, repeated reaming, poor cement jobs, and intermediate casing impairment.

Geothermal formations are commonly under-pressured, with differential pressure (the difference between the hydrostatic pressure of the drilling fluid column and the formation-pore pressure) usually above 3.4 MPa. If the surge pressure when drill pipe is tripping downhole is added, which is commonly around 3.4 MPa, which gives a total value of 6.9 MPa of sealing pressure (or differential pressure) as a reference value for geothermal applications [1].

Goodman [16] conducted a study of how the geothermal industry addressed mud losses during drilling operations. After an extensive survey, Goodman observed that geothermal operators used

[1]Corresponding author.

Contributed by the Petroleum Division of ASME for publication in the Journal of Energy Resources Technology. Manuscript received October 14, 2021; final manuscript received November 13, 2021; published online December 14, 2021. Editor: Hameed Metghalchi.

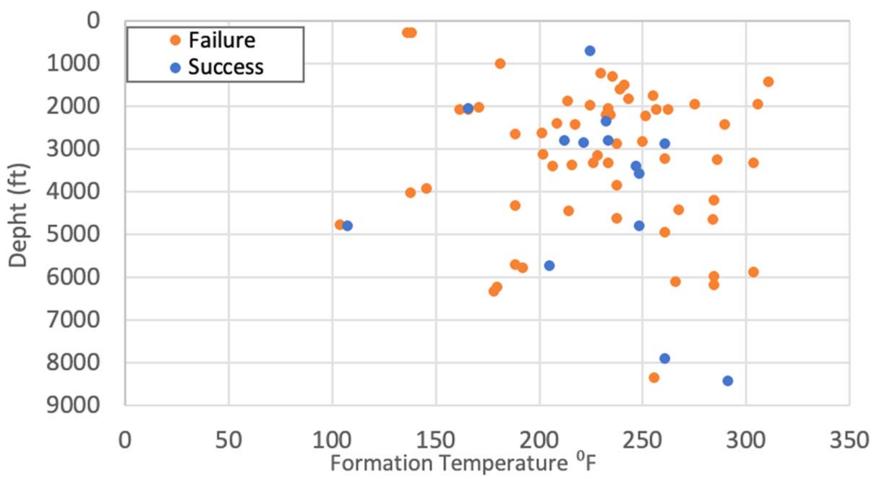

Fig. 1 LCM treatments effectiveness from temperature versus depth perspective (plot generated with information adapted from Cole et al. [8])

traditional O&G drilling approaches to solve drilling fluid losses (LCMs, pills, or cement plugs). The study revealed that, depending on the individual downhole conditions, these approaches may or may not be effective in resolving impaired circulation. Hyodo et al. [17] analyzed close to 4500 lost circulation events in Japan. In that study, 65% of the wells presented total losses, and when those losses were treated with LCM, the success rate was about 10%. At present, despite the evolution of LCM materials, these treatments' success rate is still low. Cole et al. [8] analyzed the mud losses in 15 wells in California. Ninety-five events in total were analyzed, and the overall success rate of all treatments with LCM was 25.3%. In general, it can be observed that partial and severe losses, the treatments have a better success rate, compared with their performance at total losses, where all LCM treatments failed. Total losses in geothermal wells are commonly attributed to fractures that are difficultly healed with LCM.

In the same study, the effect of temperature and depth was analyzed. In Fig. 1, LCM treatments are showed by depth and formation temperature. The temperature range of the data analyzed is between 37.8 °C and 154.5 °C. Paper, cottonseed hulls, nutshells, and calcium carbonate were used in 87% of all events. According to interviews with drilling operators presented in the study, the LCM components were mostly selected on a well-by-well basis through trial and error rather than formation properties. The severity of losses provided operators an indication of whether materials should perform well based on previous experience.

1.1 Lost Circulation Materials. In general, geothermal drilling operators have available LCMs at the rig site for immediate usage once mud losses are present. The materials are incorporated into the mud system and circulated downhole to control the losses, making LCM the first defense line operators prefer [1].

Caenn et al. [18] divided lost circulation materials (LCMs) into four categories summarized in Table 1.

As observed, LCMs are diverse in shape, density, or stiffness, and depending on their individual attributions, they work differently in reducing or avoiding drilling fluid get into the formation.

1.2 Experimental Research on Lost Circulation Materials. Extensive experimental research has been performed to evaluate the performance of LCMs. Although some experimental studies have been performed at room temperatures, they have been fundamental to understanding the sealing mechanisms. Others have tried to evaluate the performance of temperature-aged LCMs to represent their performance at geothermal conditions, but the tests are performed at room conditions. Few experimental studies have been performed measuring properties directly at high temperatures. This is due to the challenges of managing temperatures of 149 °C and above. HPHT research limitations include high pressures (necessary to avoid evaporation), very long heating and cooling times, or testing equipment wear (especially elastomers).

Howard and Scott [19] made an experimental study of different LCM performances at dynamic conditions and room temperature. They measured the sealing capability (a seal capable of holding 6.9 MPa of differential pressure) using different fracture sizes versus material concentration (Fig. 2). One of the outcomes of that experimental study is that granular materials are more effective for closing the largest fractures (up to 5000 mm). Besides,

Table 1 Lost circulation materials classification

LCM Type	Examples	Characteristics
Fibrous materials	Sawdust, cedar fiber, shredded cane stalks, micronized cellulose, bagasse, cotton fibers, shredded automobile tires, wood fibers, paper pulp	• Flexible materials • Variable sizes • Tend to be squeezed into wide openings
Flaky materials	Wood chips, shredded cellophane, mica flakes, plastic laminate	• Flat shape • Large surface area • It can form a filter cake or can be squeezed into openings
Granular materials	Calcium carbonate, ground nutshells, granular marble, Formica, corncobs, cotton hulls, granular graphite	• Chunky granular shape, with a variety of grain sizes • Strong and stiff materials • Ideal materials are insoluble and inert inside the mud
Slurries	Hydraulic cement, diesel oil-bentonite-mud mixes, and high filter loss muds	• Designed to harden with time

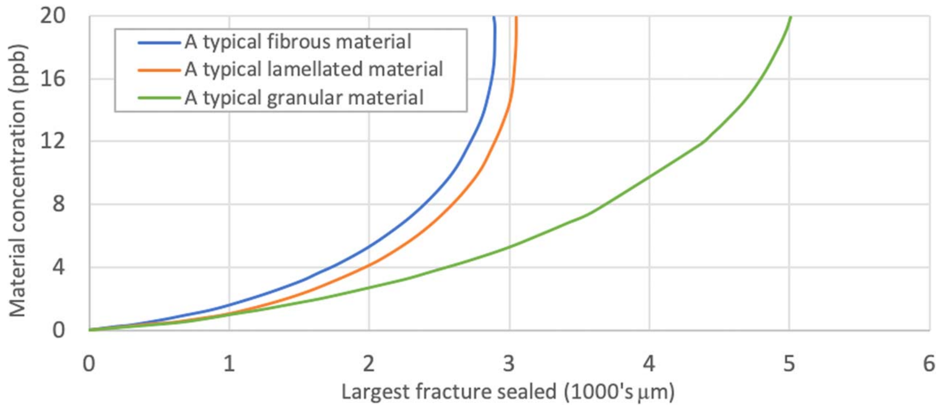

Fig. 2 Effect of LCM concentration at different fracture sizes (modified from Howard and Scott [19])

Table 2 Comparison of percentage of successful 6.9 MPa sealing pressures at different concentrations

	Cotton seed hulls			Kwik-Seal			Ruf-Plug		
Slot size, mm	5 ppb	10 ppb	Dif	5 ppb	10 ppb	Dif	5 ppb	10 ppb	Dif
1.5	66.7%	100.0%	33.3%	100.0%	100.0%	0.0%	66.7%	100.0%	33.3%
2	37.5%	100.0%	62.5%	33.3%	100.0%	66.7%	0.0%	11.8%	11.8%
3	6.7%	20.0%	13.3%	11.8%	45.5%	33.7%	0.0%	0.0%	0.0%
4	0.0%	0.0%	0.0%	0.0%	54.5%	54.5%	–	0.0%	–
5	0.0%	7.7%	7.7%	0.0%	23.1%	23.1%	–	0.0%	–

researchers found that granular LCM requires less material concentration to seal similar size fractures compared with fibrous and flaky LCMs.

Hinkebein et al. [1], in another experimental study, analyzed three cellulosic materials: cottonseed hulls, Kwik-Seal (a combination of granular, fibrous, and flakes components), and Ruf-Plug (ground corn cobs). Paper pulp was also tested, but due to poor results, it was dropped from the study. All materials were tested with a low-density drilling fluid (8.8 ppg), compounded by water and Wyoming bentonite. According to the results presented, derived from extensive laboratory experiments (223 experiments), the increasing LCM concentration in all three materials increases the likelihood of successful sealing (Table 2). However, they found that the rising LCM concentration for the materials tested does not irrevocably increase the sealing pressure. The conclusion was due to the randomness of the results, where the same type of material was tested under the same conditions, and sealing pressures cannot be replicated.

In the same research, the effect of temperature was analyzed. In this case, the materials were hot rolling aged at different temperatures (Fig. 3). The results show that all materials at room temperature managed to seal the 0.06″ (1524 μm) fractures, reaching 6.9 MPa of sealing pressure. However, when materials were tested after being hot-rolling at 204.5 °C, cottonseed hulls and Ruf-Plug LCM failed to seal the fracture, and the Kwik-Seal lost 30% of its sealing pressure strength. These results suggest that thermal degradation of LCMs properties affects their sealing performance.

1.3 Bridging and Sealing.

The process in which LCM is utilized to cure mud losses has been analyzed for years. The general perception is that LCM creates a restriction that avoids or at least reduces fluid loss by plugging the pores and fractures in the borehole. However, this conception overlooks the physics behind how the LCM works. Consequently, frequently the usage of LCM is based on trial and error or based on experience rather than as a product of an optimization analysis.

The life cycle of how LCM work can be divided into four stages: dispersion, bridging, sealing, and sustaining [20].

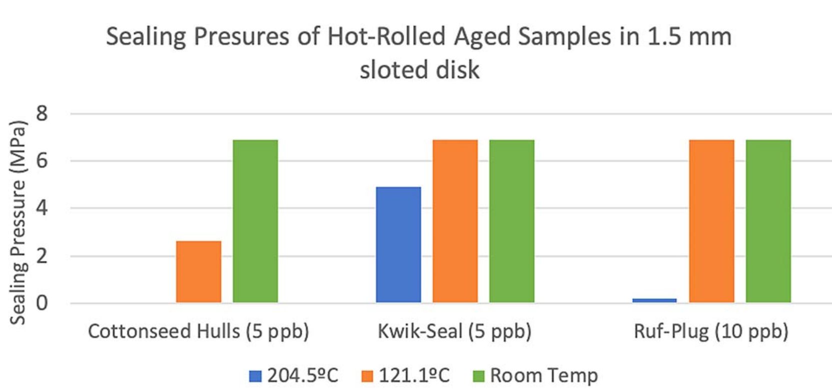

Fig. 3 Sealing pressures of three cellulosic LCM products at different temperatures (plot generated with information adapted from Hinkebein et al. [1])

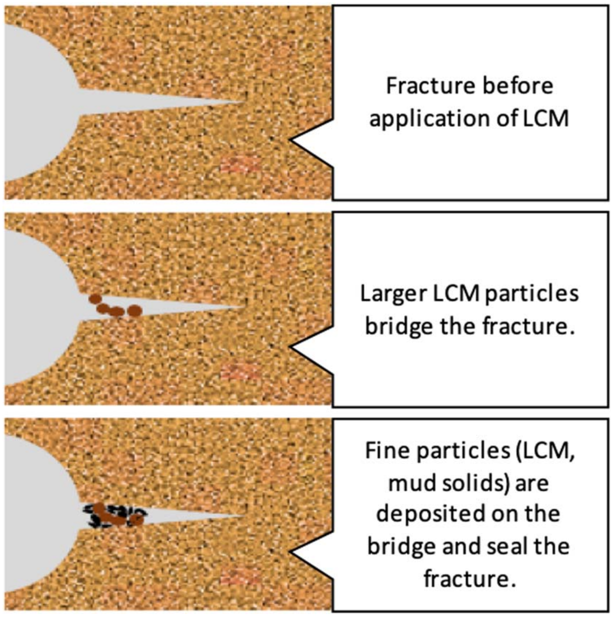

Fig. 4 LCM bridging and sealing process (adapted from Lavrov [20])

Dispersion is how the LCM arrives at the fracture. The LCM must overcome various restrictions during its journey through the mud pits and pumps system, the journey through the drill pipe, and the restrictions of the different components of the BHA until it reaches the fracture.

Bridging consists that once LCM gets into the fracture, they start forming a permeable layer across the fracture, robust enough to withstand the pressure gradients, and hold smaller particles that will create the seal (Fig. 4).

Sealing is the process in which the small particles, either undersized LCMs or mud solids (e.g., bentonite, barite), accumulate on the bridge built by the coarse LCM, filling all the spaces of the bride, generating an impermeable layer, a seal, that prevents fluid continue passing through the fracture.

Sustaining is fundamental since the seal generated by LCM needs to withstand mechanical loads and differential pressure enough time to permit drill through the theft zone, case, and cement the well.

Understanding the process is important for a successful sealing strategy. One of the most important factors is the size of the LCM. If the bridging material is larger than the fracture width, the sealing will be formed outside the fractures' mouth. This is undesirable since the drilling action can easily remove it. In contrast, if LCM is too small compared to the fracture size, it cannot effectively build a bridge [20]. As fractures in geothermal wells can vary in size, and LCM strategy may consider diverse particle sizes. A particle size distribution (PSD) analysis is essential.

Table 3 Summary of LCM selection by particle size (after Alsaba et al., 2016)

Method	Selection criteria	Authors
Abrams rule	D50 ≥ 1/3 the formation average pore size	[21]
D90 rule	D90 = the formation pore size	[23,24]
Vickers method	D90 = largest pore throat D75 < 2/3 the largest pore throat D50 ≥ 1/3 D25 = 1/7 the mean pore throat D10 > the smallest pore throat	[25]
Halliburton method	D50 = fracture width	[26]
Alsaba method	D50 should be ≥ 3/10 the fracture width D90 should be ≥ 6/5 the fracture width	[22]

The connection between the particle size of an LCM and its capability to bridge fractures has led to the development of different methods to select the proper particle size.

One of the most accepted criteria was proposed by Abrams [21]. The method consists of two rules for selecting bridging material. The first rule is that the particle size's mean size must be equal to or greater than one-third of the mean of the rock pore size. The second rule is that the sealing material must be no less than 5% of the drilling fluid volume.

Since then, different criteria have been proposed. They are summarized in Table 3. The downside of the earlier methods is that they are based on pore size. However, they have been used as selection criteria for sealing fractures. Alsaba et al. [22] proposed a new selection criterion based on a statistical analysis of extensive experimental research. LCMs with diverse particle size distributions were tested on fractures from 1000 μm to 3000 μm.

1.4 Wellbore Strengthening.

An evolution to the traditional LCM addition to the mud system is the concept of wellbore strengthening. This consists of LCM usage to intentionally increase the fracture gradient of a wellbore by adding LCM to bridge and seal fractures near-wellbore [27]. Three physical models describe the wellbore strengthening concept and how they enhance the wellbore strength in drilling operations: stress cage model, Fracture Closure Stress (FCS) model, and Fracture Propagation Resistance (FPR) model [28].

The concept of stress cage was introduced in Ref. [29], and it explains how mud additives help to seal fractures induced during drilling. The stress caging theory is to place solids at or close the mouth of a recently drilling-induced fracture that will serve to build a bridge. The bridge creates the support to hold particles that generates the seal, insulating the drilling fluid pressure from the rest of the fracture. If the seal is successful, the fluid pressure of the isolated portion of the fracture will be dissipated to the pore pressure. Then, the fracture, without the pressure that maintains it open, will close. This process increases the hoop stress around the wellbore beyond its original value.

In the FCS model, a fracture in the wellbore is generated and widened, expanded in length but not in width. LCM is forced to fill the fracture. LCM starts to accumulate inside the fracture, and as the carrier fluid is filtrating into the formation, it creates an "immobile mass" within the fracture. The immobile mass holds the fracture open and isolates the fracture end from the drilling fluid pressure. Fracture is getting more difficult to open due to increased fracture closing tension and the fracture end isolation [30].

In the FPR model, at a difference of FCS and stress cage models, the hope stress is not increased [28]. Instead of that, the idea is that a mud cake generates an impermeable layer that prevents the drilling fluid pressure from expanding the fracture [31].

2 Materials and Methods

This experimental study consisted of screening different LCMs to evaluate their capability of sealing fractures at HT and their thermal stability when incorporated into a geothermal base formula. The main challenges are related to the thermal degradation of rheological and filtration properties.

Table 4 presents the lost circulation materials tested. LCMs have a wide range of sizes, shapes, densities, and textures. This provides a comprehensive LCMs range to identify characteristics that made some materials more suitable to geothermal conditions than others. The materials presented are ready to use and required no preparation.

For the static filtration tests, the equipment used was an HPHT permeability plugging tester (PPT). This equipment is designed for performing filtration tests avoiding LCM settling. This is because the slotted disc (disc with simulated fracture) and the

Table 4 Lost circulation materials selected for the experimental study

Walnut fine	Walnut Medium	Sawdust	Altavert	Graphite Blend	Bentonite Chips
				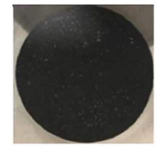	
Granular Non-deformable LCM Chemical inert Biodegradable SG: 1.25-1.30	Granular Non-deformable LCM Chemical inert Biodegradable SG: 1.25-1.30	Flaky/Fibrous Deformable LCM Temporary temperature degradable SG: 0.4-0.6	Fiber Deformable LCM Hole sweep additive Temporary temperature degradable	Granular Non-deformable LCM Blend with different sizes Torque reducing material SG: 2.19–2.26	Granular Deformable LCM Non-toxic SG: 1.11-1.14 (dry)
Micronized Cellulose (MICRO-C)	Magma Fiber Fine	Diatomaceous earth/ amorphous silica powder (DEASP)	Cotton Seed Hulls	Calcium Carbonate	Cedar Fiber
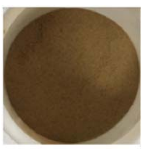	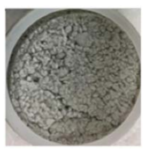	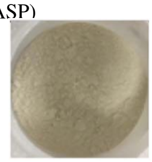			
Granular Deformable LCM Water-insoluble Cellulosic Material SG: 1.3	Fiber Deformable LCM Acid soluble Non-fermenting and non-corrosive SG: 2.6	Granular Non-deformable LCM Silica powder Squeeze pill design	Fiber Deformable LCM Biodegradable Temporary temperature degradable SG: 0.24	Granular Non-deformable LCM Acid soluble A blend of three sizes: 200, 80, and 30 CC SG: 2.75	Fiber Deformable LCM Water-insoluble Cellulosic Material SG: 0.6

collecting assembly are placed at the pressure cell top. For this study, the equipment was operated at 149 °C for the LCM screening.

Finally, for granular materials, PSD tests were performed. For PSD analysis, we used a laser diffraction particle size analyzer. The particle size measured in this equipment ranges from 0.375 μm to 2000 μm. This equipment was used for measuring PSD in dry samples.

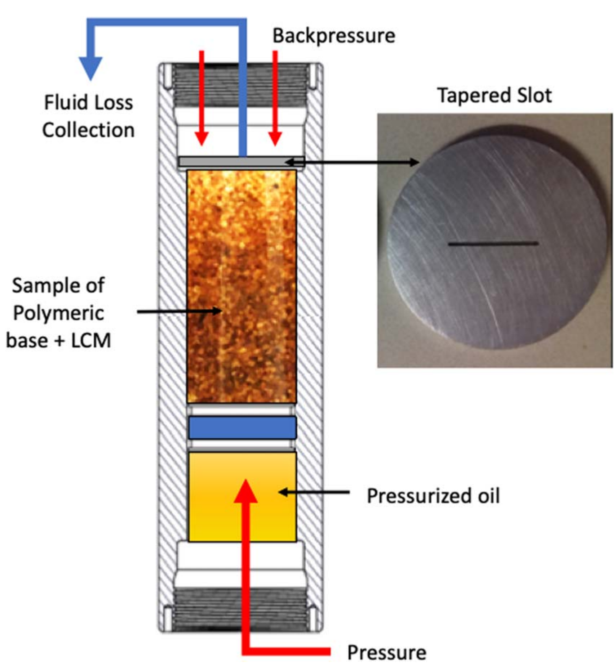

Fig. 5 Diagram of the pressure cell of the PPT apparatus for LCM filtration screening

3 Description of Tests, Results, and Analysis

Different kinds of tests have been used to evaluate the effectiveness of LCM's for sealing fractures. However, they involved the usage of complex flow loops or the modification of filtration equipment. The downside of these approaches is that the results are hard to replicate or compare unless the same flow loop/equipment is used. In this research, an un-modified PPT equipment is used, with a slotted disk to simulate a fracture (Fig. 5). The novelty of the process is using a solids-free mud; in this case, distilled water with an HPHT polymer. The polymer is a commercial polymer that ¨activates¨ with temperature, providing enough rheology to keep the LCM in suspension.

The advantage of using a free of solids mud for the test is that the sealing action is directly generated by the LCMs, providing an advantage for individual evaluation of each material sealing performance. The HPHT polymer was activated using the PPT cell, heating it to 149 °C. In Fig. 6, the mud (*a*) before and (*b*) after heating is presented. Before heating up, the mud has the minimal capability to keep LCM in suspension, then the LCM sag. After heating the mud, its rheology increased, and solids can be maintained in suspension. This is advantageous since the fluid keeps its solids' carrying capacity at high temperatures in a static condition. The free of solids mud was also tested at the same conditions without LCMs showing no sealing capacity with open fractures. Then, any sealing action is generated by the LCM itself.

The mud was prepared with distilled water and 3% in weight of the HPHT polymer. The mud was then aged for 24 h and heated up to 176.7 °C at 3.45 MPa for activation. Once the mud is activated, it was mixed with the LCMs. The mud mixed with LCMs is aged for 24 h before being tested in the PPT apparatus. The disc with the

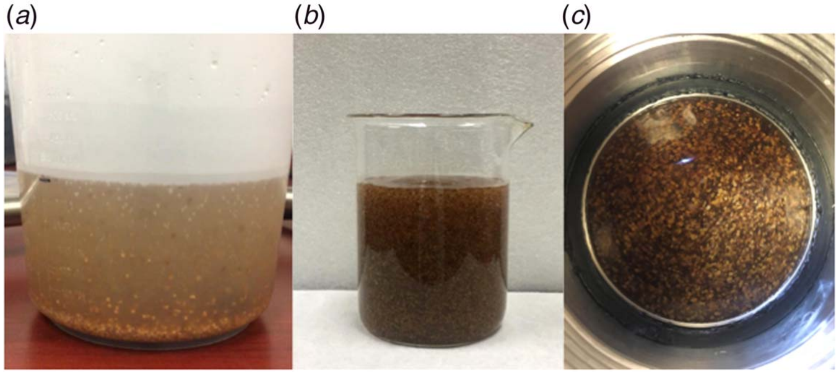

Fig. 6 Walnut fine mixed with free of solids mud: (*a*) walnut settling in mud non-thermally activated, (*b*) walnut evenly distributed in thermally activated mud, and (c) top of the PPT pressure cell filled with mud + LCM

Table 5 Materials and concentration of the base formulation

Lost circulation material	Concentration
Walnut fine	15 ppb
Walnut medium	15 ppb
Sawdust	1 ppb
Altavert	0.5 ppb
Graphite blend	15 ppb
Bentonite chips	15 ppb
MICRO-C	5 ppb
Magma fiber fine	8 ppb
DEASP	8 ppb
Cotton seed hulls	12 ppb
Calcium carbonate	20 ppb

1000 mm fracture was selected for this initial screening to evaluate each LCMs performance.

To this base formula, there were added the different LCM products at different concentrations. The concentration of each material is presented in Table 5.

The LCMs screening experiments used a similar methodology to the one presented by Savari et al. [32]. The purpose is to measure the filtration for 30 min. Once it is confirmed that the LCM can hold a sealing with mud pressure of 5.5 MPa and backpressure of 2.1 MPa, then the pressure is raised by hundreds until the sealing is lost. The maximum sealing pressure obtained is recorded (this is the differential pressure of the pressure and the back pressure).

3.1 Filtration Tests. In Fig. 7, the 30 min filtration profile results of the different tests are presented. The LCM's that performed best were MICRO-C, calcium carbonate blend, and graphite blend. What is similar to these materials is that they are granular, with small particle size, and all of the three are blends, so they have a wide range of particle size.

In Fig. 8, it is presented the 30-min filtration test and the maximum sealing pressure for each LCM. The maximum sealing pressure was obtained by the graphite blend, calcium carbonate, Altavert, and MICRO-C.

In Fig. 9, it is presented a close-up view of the 1000 μm fracture of the three materials that performed best in the filtration experiment. The three LCMs successfully sealed the fracture without other solids. The graphite blend was the only LCM that reached the maximum sealing pressure of 8.3 MPa. This value could be higher, considering that the maximum mud pressure was limited to 10.3 MPa for safety reasons (and the back pressure was a constant 2.1 MPa). The calcium carbonate blend provided a sealing pressure of 6.2 MPa. When the pressure was increased above 6.2 MPa, the sealing pressure was suddenly lost, and it was not possible to recover it back. The MICRO-C sealing pressure was 4.8 MPa. When the sealing pressure was increased above 4.8 MPa in the MICRO-C test, the sealing pressure was reduced gradually, but with time, the sealing was recovered, and pressure could be increased again to MPa. This effect can be visualized in Fig. 9, where it can be seen that in the $CaCO_3$ experiment, the seal was lost, and the fracture was open. In contrast, the MICRO-C sealing was maintained. This effect can be attributed to the deformability of MICRO-C and the non-deformability of $CaCO_3$.

3.2 Particle Size Distribution Tests. To better understand the influence of LCMs particle size, a PSD analysis was performed on

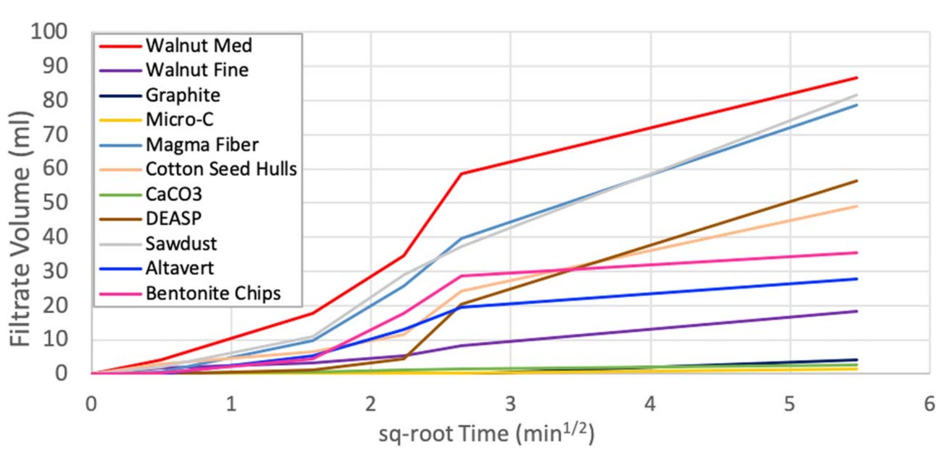

Fig. 7 Filtration results of individual tests of the free of solids mud + LCMs

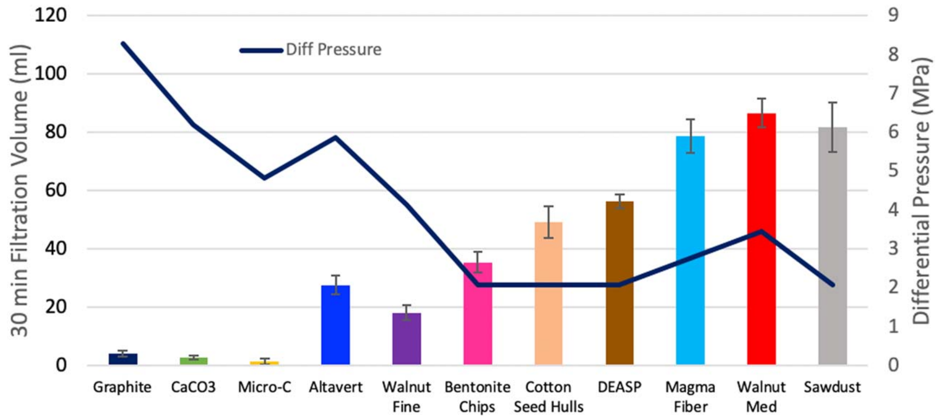

Fig. 8 Filtration volume and maximum sealing pressure obtained of different LCMs

Fig. 9 Close-up view of 1000 μm fracture once the disk was removed from the pressure cell

fine granular materials. The importance of the PSD analysis is that particle size distribution affects the performance of LCM for lost circulation treatments [7,33]. The PSD equipment measures particles from 0.375 mm to 2000 mm. Figures 10 and 11 show the test results made on the calcium carbonate blend, DEASP, MICRO-C, and graphite blend.

As it can be observed in the PSD analysis, the DEASP curve shows a Gaussian distribution of the values (bell shape), and the other materials presented a wider range of particle diameters with their curves right-skewed. To determine the influence of the PSD in the filtration performance, the filtration results of the components analyzed are presented in Fig. 12.

According to the filtration results, the materials with a wider particle size distribution (graphite blend, calcium carbonate, and MICRO-C) are the best filtration performance materials. In contrast, the DEASP, the granular material with smaller particle diameter values, had a higher filtration volume. Having a wide range of particle sizes is a desirable condition in an LCM for sealing fractures; larger grains can build the bridge, creating support for the smaller particles that generate the effect of sealing. In Table 6, it is summarized the PSD test values. The mean diameter of the DEASP is 15.67 mm, which is significantly smaller than the average diameters of the other LCMs analyzed.

4 Discussion

After analyzing the experimental results, it was identified that materials that performed better in the filtration tests were fine granular, blended materials. This does not necessarily mean that they are the best materials for all applications. However, the testing conditions show that those materials are suitable for geothermal environments.

Fine granular materials behave better at high temperatures compared with coarse larger size granular materials and fibers. A reasonable argument is that smaller particles have a larger surface area per unit of mass, meaning that the heat is distributed in a larger surface area at high temperatures, making these materials more thermally stable. That means small granular materials can keep their sealing properties at HT better than fibers and coarse materials.

For sealing a fracture, it is beneficial to have a large size range. Larger particles create a permeable bridge, and the smaller particles fill out the bridge spaces to build a seal. This can explain why LCMs like calcium carbonate and graphite blends or MICRO-C, with a wide range of particle diameters, worked better than the DEASP. The variance of DEASP (348.3 μm^2) is significantly smaller than the variance of the other LCM that present the best performance in the filtration tests.

As the filtration tests were performed with a free of solids mud, all the sealing action came from each LCM. However, in practice, drilling fluids contain solids from the mud additives and the drilling cuttings. The mentioned solids also contribute to the fracture sealing process.

The ratio between the size of the fracture and the particle size is another important factor to consider. In Table 7, it is summarized the particle size distribution of the fine granular materials analyzed. The particle sizes obtained were evaluated based on the different particle size criteria used in the industry (Table 3). In Table 8, it is presented if each of the LCM analyzed meets (Yes) or does not meet (No) each LCM selection criteria examined.

There are no selection criteria from Table 8 that calcium carbonate blend, graphite blend, and MICRO-C together completely meet. Graphite blend meets most of the conditions of the different

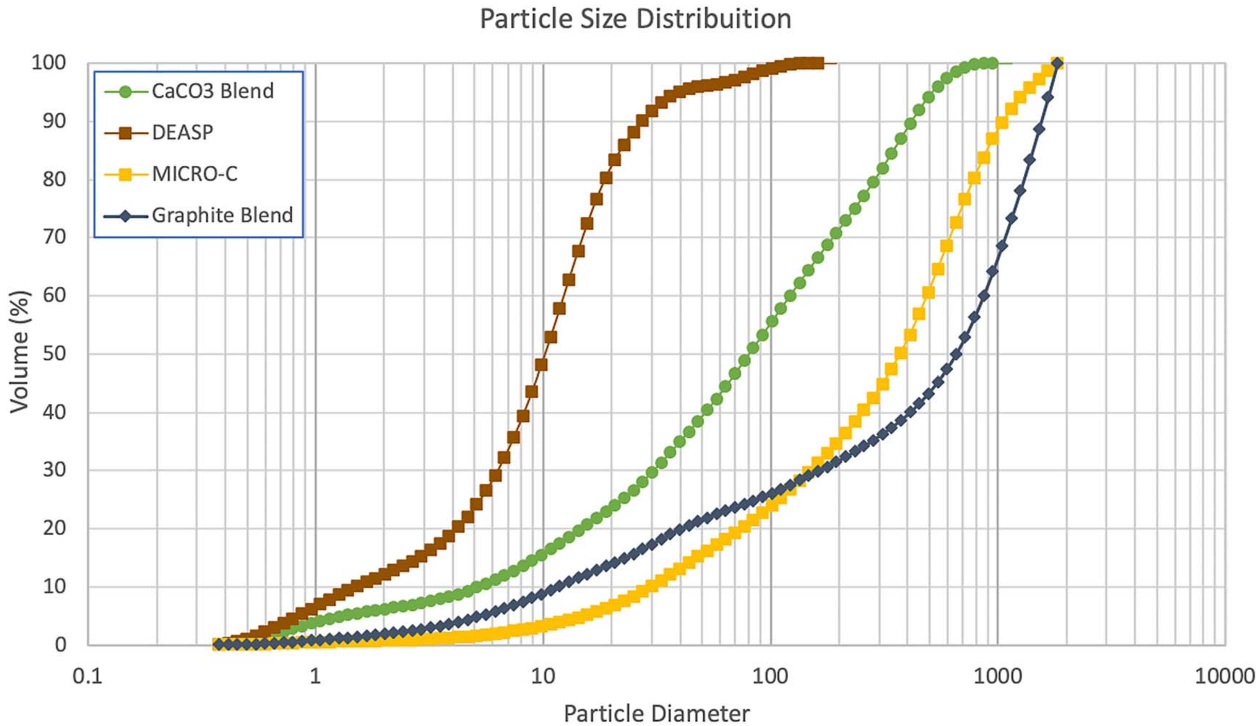

Fig. 10 PSD test on different fine granular LCMs

selection criteria presented. MICRO-C also meets most of the criteria except Vickers and Halliburton methods. Compared with the Halliburton Method, the requirements in the D50 is 500 μm and the MICRO-C D50 is 407 μm.

Sealing a fracture involves the LCM's ability to build a bridge inside the fracture. The D90 size is considered in some of the recent selection criteria. The D90 includes the largest size particles destined to bridge the fractures. As observed, MICRO-C and graphite blend met some of the D90 size criteria methods used in the industry. However, the calcium carbonate blend, LCM that showed a good performance in the filtration test, did not meet most of the criteria methods.

Calcium carbonate blend has a D90 size of 456.51 μm, close to half of the fracture width size (1000 μm). Since calcium carbonate

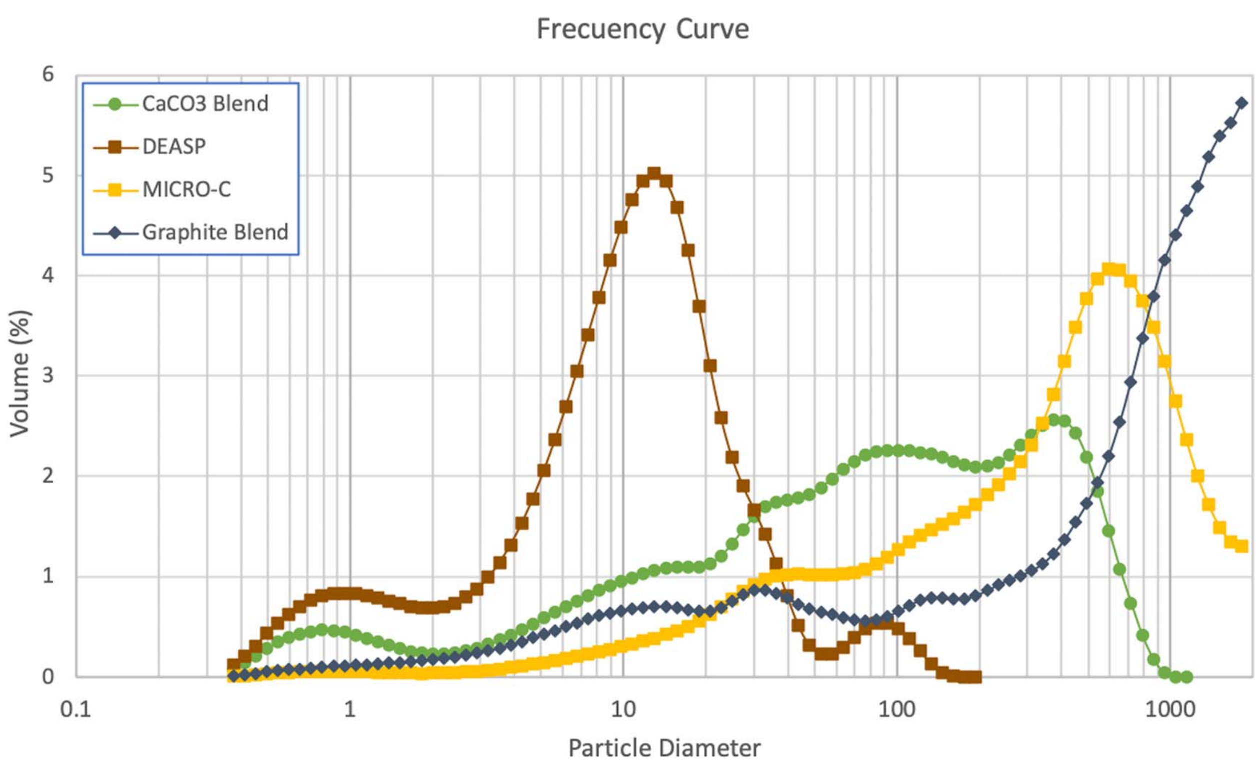

Fig. 11 Frequency curve of particle diameter test on different fine granular LCMs

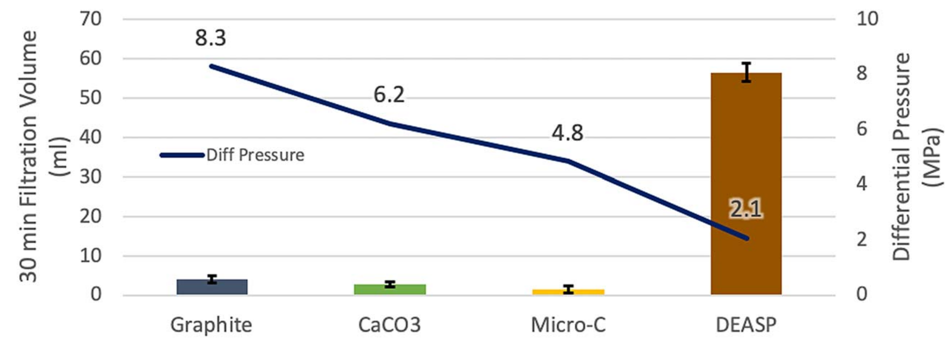

Fig. 12 Filtration and differential pressure results of fine granular LCMs tested

Table 6 Summary of PSD test on various LCM's

Variable	$CaCO_3$ blend	DEASP	MICRO-C	Graphite blend
From (μm)	0.375198	0.375198	0.375198	0.375198
To (μm)	2000	2000	2000	2000
Volume	100	100	100	100
Mean (μm)	165.78	15.67	505.66	761.21
Median (μm)	88.24	11.21	406.97	717.12
Mean/median ratio	1.88	1.40	1.24	1.06
Mode (μm)	390.96	13.61	623.27	1908.87
S.D. (μm)	186.50	18.66	452.19	632.72
Variance (μm^2)	34,782.60	348.30	204,476.00	400,336.00

Table 7 Summary of PSD analysis for fine granular materials

Material	Fracture Size	D10 μm	D25 μm	D50 μm	D75 μm	D90 μm
CaCO3 Blend	1000 μm	5.71	24.42	88.24	256.31	456.51
DEASP	1000 μm	1.65	5.81	11.21	18.21	29.87
MICRO-C	1000 μm	32.59	119.47	406.97	758.07	1153.87
Graphite Blend	1000 μm	12.77	95.11	717.12	1297.28	1696.26

Table 8 Summary of application of particle size selection methods based on the material's PSD results

Method	Selection criteria	$CaCO_3$ blend	MICRO-C	Graphite blend	DEASP
Abrams rule [21]	D50 ≥ 1/3 the formation average pore size	No	Yes	Yes	No
D90 rule [23,24]	D90 = the formation pore size	No	Yes	Yes	No
Vickers method [25]	D90 = largest pore throat	No	Yes	Yes	No
	D75 < 2/3 the largest pore throat	Yes	No	No	Yes
	D50 ≥ 1/3	No	Yes	Yes	No
	D25 = 1/7 the mean pore throat	No	No	No	No
	D10 > the smallest pore throat	–	–	–	–
Halliburton method [26]	D50 = fracture width	No	No	Yes	No
Alsaba method [22]	D50 should be ≥ 3/10 the fracture width	No	Yes	Yes	No
	D90 should be ≥ 6/5 the fracture width	No	Yes	Yes	No

successfully sealed the fracture, the D90 size value in some of the selection criteria could be re-evaluated in the future.

This suggests that 10% of the particles with size near the half of the fracture are enough to build the bridge into the fracture. Then, it is possible to distribute the remaining 90% to create a wider range of particle size. Once the bridge is built, a wider range of smaller particles will fill the permeable bridge spaces to generate the sealing.

This is an important condition since, in geothermal applications, large fractures are frequently found. In this case, materials with greater particle size need to be included. However, if the particle size is unnecessarily large, they will become prone to degrade/fail at high temperatures.

According to the experimental results, we suggest that size selection criteria must have at least two conditions. The first is that the D90 has enough size to build the bridge. The second condition is that LCM needs to have a large size distribution. This will help to generate the seal. This experimental research suggests that the PSD variance could be considered to guarantee a large particle distribution.

5 Conclusions

A methodology of screening lost circulation materials is presented by an innovative way to use the PPT at high temperatures. The usage of free of solids mud permits identifying the capability of different LCMs to seal an open fracture at HT and determine their sealing pressure in controlled conditions.

It was identified that materials that performed better in the filtration tests were granular, blended materials. Graphite blend, MICRO-C, and calcium carbonate blend sealed the 1000 mm fracture, generating sealing pressure.

Fibrous materials, such as sawdust, magma fiber, cottonseed hulls, and coarse granular materials such as walnut medium and fine, presented a lower performance than fine granular materials.

Based on the experimental findings, it is proposed that the size selection criterion must have at least two conditions. The first is that the D90 is big enough to create a bridge. The second criterion is that the LCM should have a wide size distribution. This is going to help create the seal. A wide PSD variance of an LCM is desirable. It indicates that a large particle distribution range is present. The range of LCM sizes should cover from larger particles for building the bridge and the smaller and well-sorted particles to seal the bridge.

Experimental research at high temperatures is helping us to identify materials that work best than others. Size, shape, and particle size distribution impact the filtration capability of LCM.

The conclusions presented were based on observations made during this research and applied to the different mud samples used in the analysis. It is important to remember that muds with different additives concentrations can have varying responses to high temperatures. However, the general behavior of mud is assumed to be roughly comparable.

Acknowledgment

The authors of this paper would like to thank U.S. Department of Energy's Office of Energy Efficiency and Renewable Energy (EERE) under the Geothermal Program Office Award Number DE-EE0008602 for funding this research. The statements made herein are solely the responsibility of the authors.

Conflict of Interest

There are no conflicts of interest.

Data Availability Statement

The datasets generated and supporting the findings of this article are obtainable from the corresponding author upon reasonable request. The authors attest that all data for this study are included in the paper. Data provided by a third party listed in Acknowledgment. No data, models, or codes were generated or used for this paper.

References

[1] Hinkebein, T. E., Behr, V. L., and Wilde, S. L., 1983, *Static Slot Testing of Conventional Lost Circulation Materials*, Sandia National Labs, Albuquerque, NM.

[2] Meng, M., Chen, P., and Ren, R., 2019, "Statistic Evaluation of Failure Criteria in Wellbore Stability With Temperature Effects," Fuel, **252**(9), pp. 730–752.

[3] Shi, Y., Song, X., Li, J., Wang, G., Zheng, R., and YuLong, F., 2019, "Numerical Investigation on Heat Extraction Performance of a Multilateral-Well Enhanced Geothermal System With a Discrete Fracture Network," Fuel, **244**(5), pp. 207–226.

[4] Ezeakacha, C. P., and Salehi, S., 2019, "A Holistic Approach to Characterize Mud Loss Using Dynamic Mud Filtration Data," ASME J. Energy Resour. Technol., **141**(7), p. 072903.

[5] Wagle, V., Kalgaonkar, R., AlYami, A., and AlKhalaf, S., 2021, "Nanosilica-Based Loss Circulation Composition to Cure Moderate to Severe Losses," ASME J. Energy Resour. Technol., **143**(10), p. 103002.

[6] Vivas, C., Salehi, S., Tuttle, J. D., and Rickard, B., 2020, "Challenges and Opportunities of Geothermal Drilling for Renewable Energy Generation," GRC 2020 Virtual Annual Meeting & Expo, Virtual Meeting, Oct. 18–23, pp. 904–918.

[7] Magzoub, M. I., Salehi, S., Hussein, I., and Nasser, M., 2021, "Development of a Polyacrylamide-Based Mud Formulation for Loss Circulation Treatments," ASME J. Energy Resour. Technol., **143**(7), p. 073001.

[8] Cole, P., Young, K., Doke, C., Duncan, N., and Eustes, B., 2017, "Geothermal Drilling: a Baseline Study of Nonproductive Time Related to Lost Circulation," Proceedings of the 42nd Workshop on Geothermal Reservoir Engineering, Stanford, CA, pp. 13–15.

[9] Snyder, N. K., Visser, C. F., Alfred, E. I., Baker, W., Tucker, J., Quick, R., and Nagle, T., 2018, *Geothermal Drilling and Completions: Petroleum Practices Technology Transfer*, National Renewable Energy Lab (NREL), Golden, CO.

[10] Marbun, B., Aristya, R., Pinem, H. R., Ramli, S. B., and Gadi, B. K., 2013, "Evaluation of Non Productive Time of Geothermal Drilling Operations—Case Study in Indonesia," Thirty-Eighth Workshop on Geothermal Reservoir Engineering, Stanford University, Stanford, CA, Feb. 11–13, p. 8.

[11] Pálsson, B., Hólmgeirsson, S., Guðmundsson, Á, Bóasson, HÁ, Ingason, K., Sverrisson, H., and Thórhallsson, S., 2014, "Drilling of the Well IDDP-1," Geothermics, **49**(1), pp. 23–30.

[12] Bolton, R. S., Hunt, T. M., King, T. R., and Thompson, G. E. K., 2009, "Dramatic Incidents During Drilling at Wairakei Geothermal Field, New Zealand," Geothermics, **38**(1), pp. 40–47.

[13] Liles, K. J., Sadler, L. Y., and Goode, A. H., 1976, *Geothermal Well Drilling Fluid Technology: A Literature Survey*, National Technical Reports Library—NTIS.

[14] Cromling, J., 1973, "Geothermal Drilling in California," J. Pet. Technol., **25**(9), pp. 1033–8.

[15] Nuckols, E. B., Miles, D., Laney, R., Polk, G., Friddle, H., and Simpson, G., 1981, "Drilling Fluids and Lost Circulation in Hot Dry Rock Geothermal Wells at Fenton Hill," International Geothermal Drilling and Completions Technology Conference, Albuquerque, NM, Jan. 21.

[16] Goodman, M. A., 1981, *Lost Circulation in Geothermal Wells: Survey and Evaluation of Industry Experience*, United States.

[17] Hyodo, M., Kitao, K., and Furukawa, T., 2000, "Development of Database System for Lost Circulation and Analysis of the Data," World Geothermal Congress, Kyushu–Tohoku, Japan, May 28–June 10.

[18] Caenn, R., Darley, H. C. H., and Gray, G. R., 2016, *Composition and Properties of Drilling and Completion Fluids*, Seventh Ed., Gulf professional publishing, Cambridge, MA.

[19] Howard, G. C., and Scott, P. P., 1951, "An Analysis and the Control of Lost Circulation," J. Pet. Technol., **3**(6), pp. 171–182.

[20] Lavrov, A., 2016, *Lost Circulation: Mechanisms and Solutions*, Elsevier Inc.

[21] Abrams, A., 1977, "Mud Design To Minimize Rock Impairment Due To Particle Invasion," J. Pet. Technol., **29**(5), pp. 586–592.

[22] Alsaba, M., Al Dushaishi, M. F., Nygaard, R., Nes, O. M., and Saasen, A., 2017, "Updated Criterion to Select Particle Size Distribution of Lost Circulation Materials for an Effective Fracture Sealing," J. Pet. Sci. Eng., **149**, pp. 641–648.

[23] Smith, P. S., Browne, S. V., Heinz, T. J., and Wise, W. V., 1996, "Drilling Fluid Design to Prevent Formation Damage in High Permeability Quartz Arenite Sandstones," SPE's Annual Technical Conference and Exhibition, Denver, CO, Oct. 6–9, Society of Petroleum Engineers.

[24] Hands, N., Kowbel, K., Maikranz, S., and Nouris, R., 1998, "Drill-in Fluid Reduces Formation Damage, Increases Production Rates," Oil Gas J., **96**(7).

[25] Vickers, S., Cowie, M., Jones, T., and Twynam, A. J., 2006, "A new Methodology That Surpasses Current Bridging Theories to Efficiently Seal a Varied Pore Throat Distribution as Found in Natural Reservoir Formations," AADE Drilling Fluids Technical Conference, Houston, TX, Apr. 11–12.

[26] Whitfill, D., 2008, "Lost Circulation Material Selection, Particle Size Distribution and Fracture Modeling with Fracture Simulation Software," IADC/SPE Asia Pacific Drilling Technology Conference and Exhibition, Jakarta, Indonesia, Aug. 25–27, Society of Petroleum Engineers.

[27] Salehi, S., and Nygaard, R., 2011, "Evaluation of new Drilling Approach for Widening Operational Window: Implications for Wellbore Strengthening," SPE Production Operations Symposium, Oklahoma City, OK, Mar. 27–29.

[28] Magzoub, M. I., Salehi, S., Hussein, I. A., and Nasser, M. S., 2020, "Loss Circulation in Drilling and Well Construction: The Significance of Applications of Crosslinked Polymers in Wellbore Strengthening: A Review," J. Pet. Sci. Eng., **185**(2), p. 106653.

[29] Alberty, M. W., and McLean, M. R., 2004, "A Physical Model for Stress Cages," SPE Annual Technical Conference and Exhibition, Houston, TX, Sept. 26–29, pp. 2867–2874.

[30] Dupriest, F. E., 2005, "Fracture Closure Stress (FCS) and Lost Returns Practices," SPE/IADC Drilling Conference, Amsterdam, The Netherlands, Feb. 23–25.

[31] Morita, N., Fuh, G. F., and Black, A. D., 1996, "Borehole Breakdown Pressure with Drilling Fluids—II. Semi-Analytical Solution to Predict Borehole Breakdown Pressure," Int. J. Rock Mech. Min. Sci. Geomech., **33**(1), pp. 53–69.

[32] Savari, S., Whitfill, D. L., Jamison, D. E., and Kumar, A., 2014, "A Method to Evaluate Lost Circulation Materials-Investigation of Effective Wellbore Strengthening Applications," SPE/IADC Drilling Conference Proceedings, Vol. 1, Society of Petroleum Engineers (SPE), pp. 538–544.

[33] Ezeakacha, C. P., Salehi, S., and Hayatdavoudi, A., 2017, "Experimental Study of Drilling Fluid's Filtration and Mud Cake Evolution in Sandstone Formations," ASME J. Energy Resour. Technol., **139**(2), p. 022912.